

New insights into the origin and evolution of glossic features in coarse-textured soils in northern lower Michigan (USA)

Christopher J. Baish | Randall J. Schaetzl 

Dep. of Geography, Environment, and Spatial Sciences, Michigan State Univ., East Lansing, MI 48824, USA

Correspondence

Randall J. Schaetzl, Dep. of Geography, Environment, and Spatial Sciences, Michigan State Univ., East Lansing, MI 48824, USA.
Email: soils@msu.edu

Assigned to Associate Editor Kyungsoo Yoo.

Abstract

Although glossic horizons are widespread throughout the Great Lakes region (USA), any type of detailed empirical investigation of their genesis has not been conducted for decades. In this study, we investigated a well-drained Haplic Glossudalf formed in calcareous till in northern Michigan and examined its glossic features across five stages of development, from nondegraded to completely degraded. Along this sequence, the glossic horizon is formed from a Bt horizon, then destroyed, evolving into an E horizon. Argillic horizon degradation is initiated from the top downward, along discrete percolation pathways. Here, temporary, highly localized, anoxic conditions favor the reduction and eluviation of Fe oxides associated with argillans. After Fe removal, clay, and to lesser extent fine silt, in the argillans become mobilized. This process results in bleached, E horizon interfingerings that penetrate the upper Bt horizon. Although eluviation of clay and fine silt is required for glossic horizon formation, their removal follows a distinct pathway from fine clay through coarse clay, and finally fine silt. This research documents the importance of redox processes at microsites in the upper Bt horizon as the destabilizing trigger for glossic horizon formation. Redox processes and microerosion may be more important than the traditionally accepted view of destabilization of clay floccules by loss of basic cations from the exchange complex. We also note that lessivage, as traditionally defined, in these soils is associated with not just clay translocation, but also fine silt.

1 | INTRODUCTION

As defined in *Soil Taxonomy* (Soil Survey Staff, 1999, 2014b), the glossic horizon is a diagnostic subsurface horizon that is ≥ 5 cm in thickness and consists of an eluvial portion (E part), which constitutes 15–85% of the glossic horizon by volume, and an illuvial portion (B part), which is usually the remnants of an argillic horizon. The eluvial portion of the glossic horizon typically occurs as irregular bodies, interfingerings,

and/or tongues (i.e., glossic features) that, when viewed in vertical cross-section, extend into the upper portion of the underlying illuvial horizon (Bockheim, 2015; Soil Survey Staff, 1999). In the World Reference Base (IUSS Working Group WRB, 2015), features exhibiting such morphology are described as *albeluvic glossae*. Current theory argues that glossic features form by the top-down degradation of the clay-enriched illuvial horizon, as clays and their associated Fe oxides are removed and translocated downward (Bockheim, 2015; Soil Survey Staff, 2014b). In order to represent the transitional nature of the glossic horizon in taxonomic description, it is distinguished with an E/B and/or B/E designation.

Abbreviations: CBD, cumulative bin difference; CEC, cation exchange capacity; LD, lithologic discontinuity; ODOE, optical density of the oxalate extract; pXRF, portable X-ray fluorescence; SOC, soil organic carbon.

About 63% of all of the soil series in the United States with a glossic horizon occur in the upper Great Lakes region, accounting for ~64,000 km² (Bockheim, 2015) (Figure 1). Such soils tend to be classified as either Alfisols (75%) or Spodosols (>24%) and are most often found on coarse-loamy (40%) or fine-loamy (22%) parent materials. Most glossic Alfisols (excluding those with aquic conditions) classify as Haplic Glossudalfs or Oxyaquic Glossudalfs, whereas most Spodosols with glossic features classify as Alfic Haplorthods or Alfic Oxyaquic Haplorthods. Many of these soils, particularly in the northern Great Lakes region, exhibit bisequal morphologies (Aide & Aide, 2020; Bockheim, 2003; Harpstead & Rust, 1964; Hole, 1975; Ranney & Beatty, 1969; Schaetzl, 1996; Weisenborn & Schaetzl, 2005). Thus, they differ from typical Alfisols and Spodosols in that they usually have spodic morphology (e.g., E-Bs, E-Bh, or E-Bhs sequa) in their upper profile, whereas their lower sequum generally resembles Alfisols (e.g., E/B-Bt). In these soils, the glossic horizons occurs as a distinct eluvial-illuvial zone at the interface between the two sequa. A typical bisequal Glossudalf has O-A-E-Bs-E/B-Bt-C horization, where the E/B horizon is the glossic horizon.

Over the past several decades, only a few studies have reported on glossic soils in the Great Lakes region (Bockheim, 2003, 2015; Schaetzl, 1996; Weisenborn & Schaetzl, 2005). In none of these studies was glossic horizon genesis the focus of detailed empirical investigation. Only two prior studies have specifically examined glossic horizon genesis in soils of the Great Lakes region, both of which date to the mid-20th century and were conducted on fine-loamy parent materials (Bullock et al., 1974; Ranney & Beatty, 1969). Thus, glossic horizon genesis in soils of the Great Lakes region, particularly those on coarse-loamy parent materials, remains largely unevaluated in terms of recent genetic models developed for similar soil types occurring in other (nonregional) glaciated locales (e.g., Jamagne et al. [1984] in France, and Payton [1993] in England). We argue that the findings from these recent studies, namely the loss of Fe as the destabilizing trigger of glossic feature genesis, may have important implications for soils containing similar pedogenic features in the Great Lakes region. Thus, to test these hypotheses, we conducted a detailed empirical investigation of a well-drained Glossudalf, formed in coarse-loamy, calcareous glacial till in northern Lower Michigan, in order to evaluate the development and evolution of its glossic horizon, and thereby develop a pedogenic model that conceptualizes the genetic processes and pathways associated with argillic horizon degradation in coarse-loamy soils. We argue that such knowledge will add to a more complete characterization of glossic soils in the Great Lakes region. Such data and study are important to advancing current theories in soil genesis, including generalized theories of lessivage, while also enhancing the classification, mapping, and management of such soils.

Core Ideas

- The glossic horizon in this study has formed by degradation of an argillic horizon.
- Degradation is initiated by localized redox processes which facilitate loss of Fe oxides.
- Eluviation of Fe destabilizes materials in illuviation cutans, facilitating further translocation.
- Translocation can occur even if the exchange complex is saturated by basic cations.
- Temporally, the loss of materials follows the pathway fine clay-coarse clay-fine silt.

2 | MATERIALS AND METHODS

2.1 | Site location and geomorphic setting

We studied a glossic soil at a site in Montmorency County, Michigan (Figure 2). Prior to the selection of this site, we conducted a series of initial field investigations at seven target locations in northern Michigan, identified in GIS, all of which were mapped as having a soil with (a) a coarse-loamy, calcareous, glacial till parent material, (b) a well-developed glossic horizon with texturally contrasting eluvial-illuvial zones, and (c) no evidence that the glossic horizon is associated with the occurrence of a lithological discontinuity. Of the seven target locations, three were deemed suitable for further analysis, having met the three criteria listed above. Of these three, one site was then chosen for detailed study because it (a) was located in state-managed woodlot, (b) showed no signs of recent anthropogenic disturbance, as evidenced by the presence of mature second-growth forest and intact surface litter horizons, and (c) was not so rugged or densely vegetated as to pose problems of access for a backhoe.

Physiographically, the site is located on a gentle (4%), north-facing backslope position of an isolated upland ridge that is part of a broader, highly dissected ground moraine complex, known locally as the Atlanta Channeled Uplands (Burgis, 1977; Schaetzl et al., 2013). The ridges are formed in thick, calcareous, coarse-loamy till and stand 20–40 m above the intervening, flat-floored, outwash dominated valleys. The Atlanta Channeled Uplands lie immediately inside of the Port Huron moraine, formed by a readvance of the Laurentide Ice Sheet at ~15,500 calibrated years before present (Blewett et al., 1993; Krist & Lusch, 2004). Thus, parent materials here became subaerial at ~15,000 yr ago, but the onset of pedogenesis may have been delayed due to postglacial permafrost (Schaetzl, 2008).

Presettlement vegetation records describe upland forests in the region, dominated by northern mixed

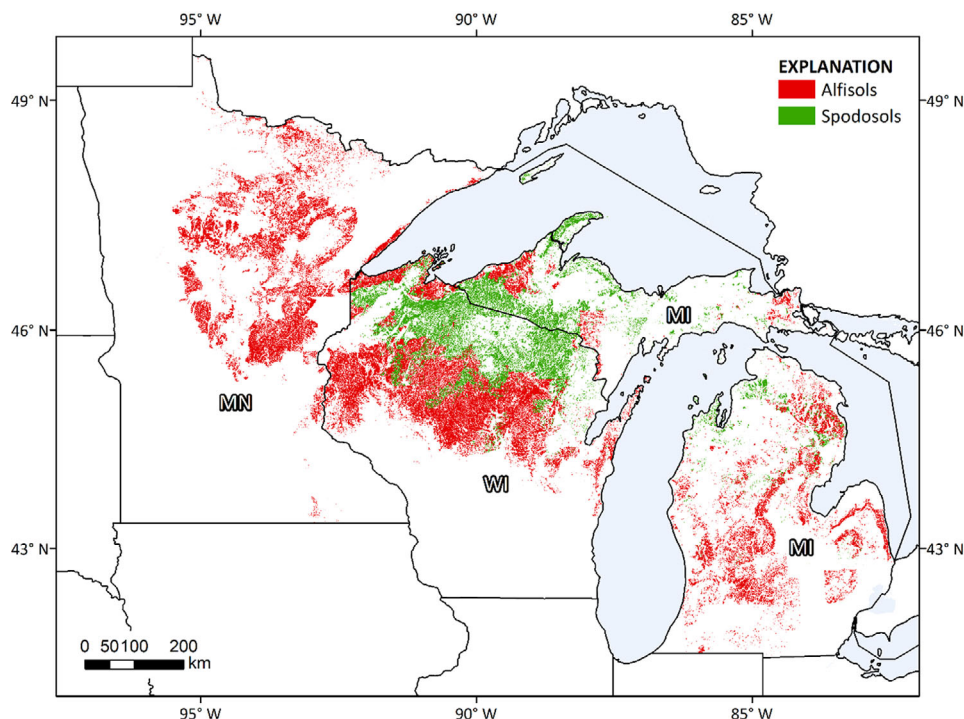


FIGURE 1 Distribution of soil series containing glossic diagnostic features in the upper Great Lakes region, split out by soil taxonomic order. Source: Natural Resources Conservation Service (NRCS) Soil Survey Geographic Database (SSURGO) data

coniferous–deciduous communities on mesic sites, and mixed-pine communities on drier sites (Comer et al., 1995). Specifically, the ridge upon at the study site was in a beech–sugar maple–hemlock [*Fagus grandifolia* Ehrh.–*Acer saccharum* Marshall–*Tsuga canadensis* (L.) Carrière] forest in the late 19th century (Comer et al., 1995). Although associated species still exist in the area today, forest assemblages have been largely altered by logging and postlogging fires (Comer et al., 1995; Whitney, 1987). At the time of sampling, the second-growth vegetative cover at the study site was dominated by quaking aspen (*Populus tremuloides* Michx.), northern red oak (*Quercus rubra* L.), red maple (*Acer rubrum* L.), and black cherry (*Prunus serotina* Ehrh.), with minor components of white pine (*Pinus strobus* L.) and paper birch (*Betula papyrifera* Marshall). The presence of mature tree cover and intact surface organic horizons suggest that erosional disturbance at the site has been relatively minimal for at least the last several decades. Evidence of recent floral or faunal bioturbation (e.g., tree uprooting or animal burrowing) was not observed at the site.

The climate in the region is cool and humid, with a frigid soil temperature regime and a udic soil moisture regime (Soil Survey Staff, 2014b). The National Weather Service Station at Atlanta (~10 km south of the site) reports an average annual precipitation of 658 mm, and mean winter (January) and summer (July) temperatures of -7.9 and 19.5 °C, respectively.

Due to its position outside (east) of the major Lake Michigan snowbelt (Andresen & Winkler, 2009; Henne & Hu, 2010), the average annual snowfall in Atlanta (171 cm) is generally less than at other nearby but more westerly sites (Eichenlaub, 1970; Henne & Hu, 2010; Isard & Schaetzl, 1995). As a result of the cold temperatures and thin snowpacks, the upper few decimeters of the soils near Atlanta are often frozen, and thus largely pedogenically and biologically inactive, for much of the winter (Isard & Schaetzl, 1995; Schaetzl & Isard, 1991). Regional modeling data suggest that infiltration values near Atlanta are greatest during the spring snowmelt period (late March through April), during which cumulative infiltration totals generally range from 120 to 140 mm (Schaetzl & Isard, 1991).

Most of the upland soils near the study site are mapped within the Millersburg series (coarse-loamy, mixed, active, frigid Haplic Glossudalfs). This series has been reported only in northern lower Michigan, where it is of moderate extent (~19,400 ha) (<https://soilseries.sc.egov.usda.gov/osdquery.aspx>). Millersburg soils are often mapped in a complex with Klacking (loamy, mixed, semiactive, frigid Arenic Glossudalfs) and Graycalm (isotic, frigid Lamellic Udipsamments) soils (Purkey, 2003). The typical Millersburg pedon has loamy sand textures and contains a weakly developed spodic-like upper sequum overlying a glossic horizon that has formed in the upper part of an argillic horizon.

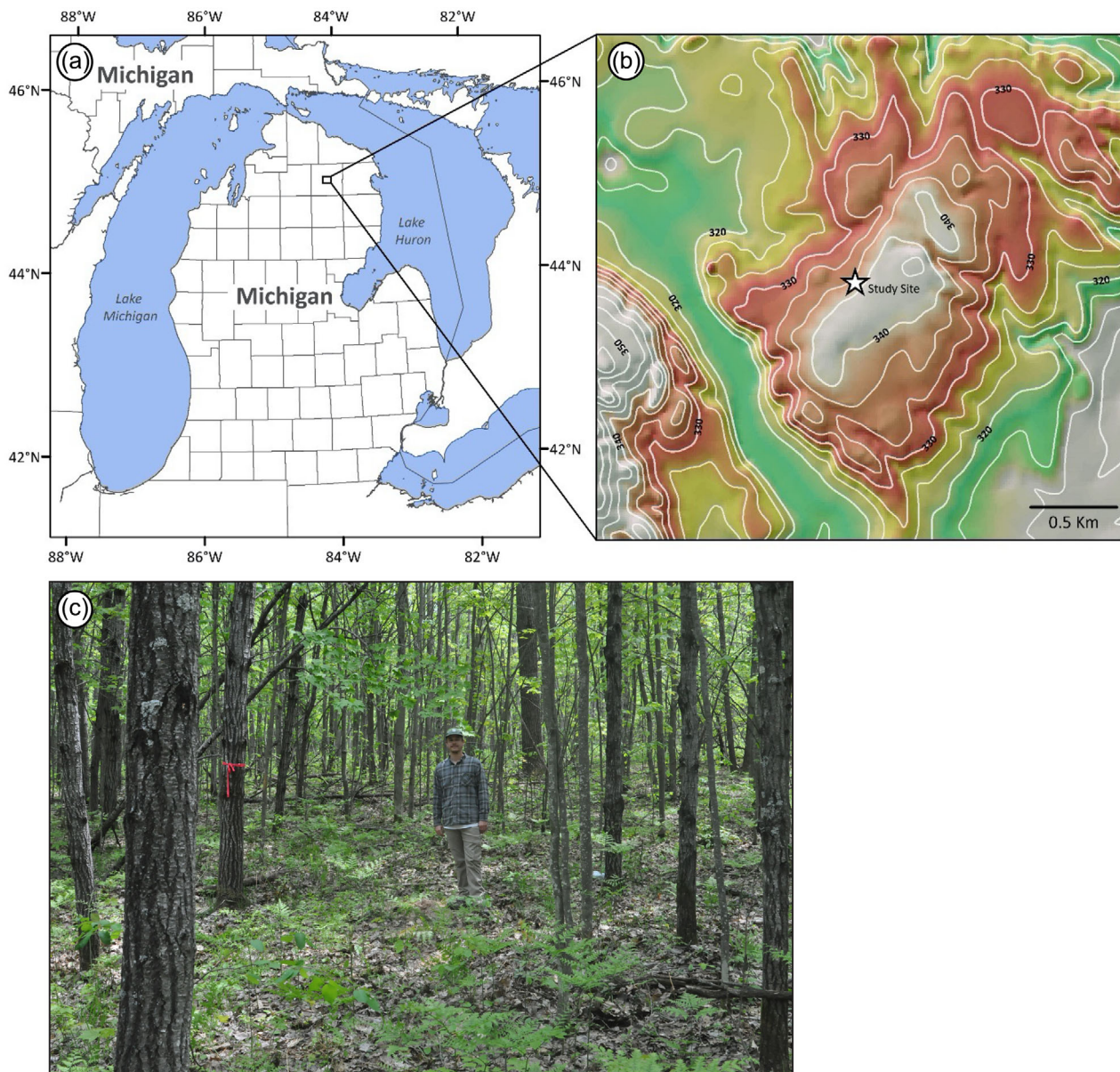


FIGURE 2 (a) General location of the study site in Montmorency County, Michigan. (b) Specific location of the study site ($\sim 45^{\circ}04'29.8''$ N, $84^{\circ}08'00.1''$ W) on a hill-shaded (10 m) digital elevation model. Contour values are in meters above sea level. (c) Photograph of the study site taken at the time of sampling, prior to soil pit excavation

2.2 | Field methods

In the field, a 2-m-deep soil pit was excavated by backhoe and the profile was described according to Natural Resource Conservation Service guidelines (Schoeneberger et al., 2012) (Figure 3). Because tills in this region are calcareous (Purkey, 2003; Schaetzl, 1996; Schaetzl, 2001), the depth to unaltered parent material was determined with dilute HCl. Bulk samples of ~ 500 g were collected from each genetic horizon and from the broader eluvial (E part) and remnant (B part) portions of the glossic (E/B) horizon. Bulk samples of undisturbed ped aggregates were also collected from select locations within the glossic horizon and the immediately subjacent,

nondegraded illuvial zone (i.e., upper Bt1 horizon). To facilitate detailed analyses of glossic horizon characteristics, namely the sequence by which eluvial (E part) soil materials in discrete soil units (peds) evolve throughout the degradational process, the ped aggregates were separated into five distinct groups, ranging from nondegraded (generally from the upper Bt horizon) to completely degraded (generally wholly albic [E part] materials), in the field (Table 1; Figure 4). Lastly, we collected core samples in duplicate from each horizon for bulk density determination (Blake & Hartage, 1986).

Samples were transported to Michigan State University for characterization; upon arrival at the laboratory, the undisturbed degradational group samples were sealed in plastic

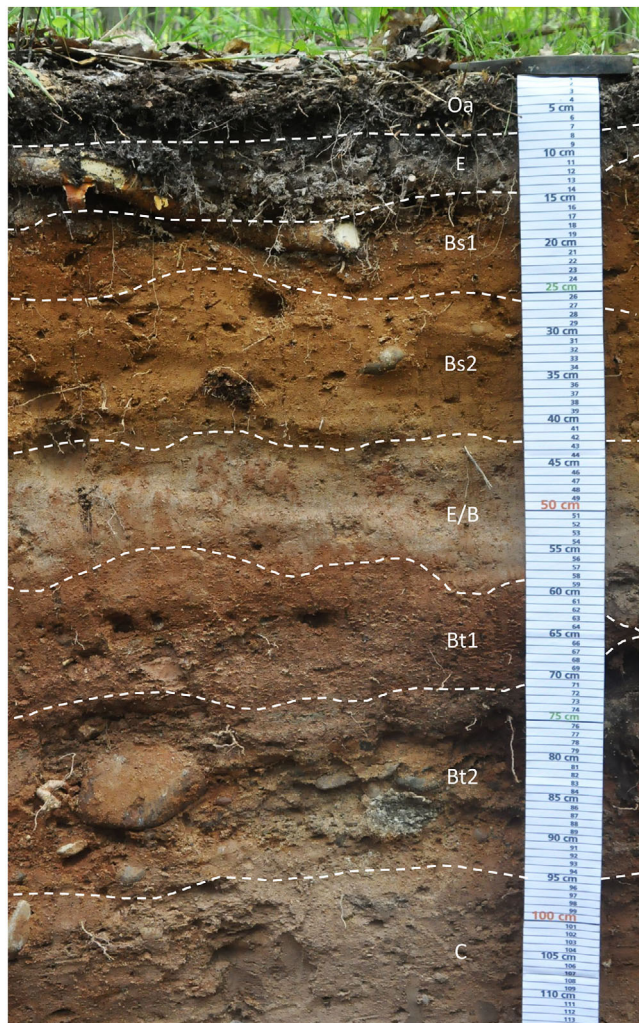


FIGURE 3 Photograph of the soil under study, with approximate horizon boundaries indicated by dashed lines

bags and stored at $\sim 5^\circ\text{C}$ to retain field-moisture conditions and to prevent structural collapse that may occur upon drying.

2.3 | Laboratory methods

All horizon-based samples were air dried for 24 h, gently disaggregated with a mortar and pestle, and sieved to 2 mm to remove coarse fragments and large organic materials. The remaining fine-earth fraction was then homogenized by passing it through a sample splitter three times in order to ensure sufficient representativeness for subsequent laboratory analyses (Schumacher et al., 1990).

Prior to the processing of degradational group samples (Figure 4), several air-dried aggregates from each group were examined under a binocular microscope, to confirm that they met the morphological criteria observed in the field. The aggregates were then carefully dissected with a scalpel under

$3\times$ magnification to isolate discrete representative subsamples from each of the degradational groups. Dissection of end-member groups (Groups I and V) was first completed to assure that the peds contained no morphological evidence of intermediate stages of degradation. Argillan materials were also collected from the faces of intact (i.e., nondegraded) Group I peds by carefully plucking the cutans from the underlying matrix material with the scalpel. Any residual skeletal particles that remained attached to the undersides of the cutans were removed by repeatedly washing the material, after gentle disaggregation, through a $50\text{-}\mu\text{m}$ mesh sieve. Dissection of intermediate groups (Groups II, III, and IV) was then undertaken to isolate eluvial (E part) soil materials, as much as possible. The peds were first halved along their long axis to expose their interiors. Eluvial soil materials were then isolated by gently scraping the exteriors of the peds. Any visible remnant (B part) materials that were detached during scraping were removed from the sample using precision tweezers. Isolated materials within each group were then combined and homogenized to create a larger, fully representative sample, from which subsamples were taken for subsequent analyses. In summary, a total of six samples were derived, including a matrix and argillan subsample from the intact illuvial (Bt horizon) zone, a matrix subsample from the completely degraded zone, and an eluvial (E part) subsample from each of the three intermediately degraded zones.

Soil textures were determined using a Malvern Mastersizer 2000E laser diffraction analyzer. Diffractometry pretreatment involved shaking subsamples (~ 0.5 g) for 1 h in a water-based solution of $(\text{NaPO}_3)_{13}\cdot\text{Na}_2\text{O}$ to disperse aggregates. For each genetic horizon sample, paired subsamples were analyzed, and the data were compared to assess for random intrasample variance according to the cumulative bin difference (CBD) method of Miller and Schaetzl (2012). The CBD is calculated by summing the absolute differences between the two subsamples for all of the 105 particle size “splits” (or bins) measured by the laser diffraction unit. Subsample pairs with a CBD of <1 standard deviation above the mean CBD of all genetic horizon subsamples were considered to be statistically similar. In instances where this threshold was exceeded, we analyzed additional subsamples until the criteria were satisfied. The mean value of the two subsamples with the lowest CBD values passing the threshold criteria was then considered the best representative textural “signature” for that horizon. For each glossic horizon group sample, a minimum of five subsamples were analyzed and the mean was considered the representative textural “signature” for that group. Because laser diffractometry tends to underestimate the clay content and overestimate the silt fraction (Eshel et al., 2004; Fisher et al., 2017; Konert & Vandenberghe, 1997; Yang et al., 2019), we defined the clay-silt textural break at $8\ \mu\text{m}$, as guided by recent studies reported in Michigan (Nyland et al., 2018; Schaetzl, Baish, et al., 2020).

TABLE 1 Description of morphological criteria used to separate glossic horizon ped samples into degradational groups

Group	Name	Description
I	Nondegraded	Wholly intact (nondegraded) material from the upper Bt horizon. Material has a reddish-brown (5YR 4/4) color and contains illuviation cutans that occur as bridges between skeletal (primary) grains and as oriented coatings on ped faces and lining pores. Little to no visible evidence of degraded, eluvial (E part) material in matrix.
II	Weakly degraded	Primarily composed of remnant (B part) material ($\geq 75\%$) with minor components of degraded, eluvial (E) material. E material occurs as thin (< 2 mm) light brown (7.5YR 6/3) rinds on ped margins and as filaments within macropores and active root channels surrounding remnant (B) material.
III	Moderately degraded	Peds composed of approximately equal portions of degraded, eluvial (E part) material and remnant (B part) material. B material has a reddish-brown (5YR 4/4) color and occurs as irregular aggregates (~ 1 – 2 cm in diam.) in ped interiors, surrounded by light brown (7.5YR 6/3) E material.
IV	Strongly degraded	Primarily composed of degraded, eluvial (E) material ($\geq 75\%$) with minor components of remnant (B part) material. B material has a reddish brown (5YR 4/4) color and occurs as small remnant aggregates (< 1 cm in diam.) in ped interiors, surrounded by light brown (7.5YR 6/3) E material.
V	Completely degraded	Peds of wholly degraded, eluvial material in the glossic (E/B) horizon. Degraded material has a light brown (7.5YR 6/3) color and occurs as coarse-textured skeletal (primary) grains. Little to no visible evidence of remnant (B) material in matrix.

Soil geochemistry was determined using a Bruker S1 Titan 800 handheld X-ray fluorescence (pXRF) analyzer, using the multiphase “Geo Exploration” mode with a scan time of 140 s at 50 keV and 35 μ A. The pXRF pretreatment involved grinding ~ 15 -g subsamples of whole-soil material (i.e., unwashed of coatings) for 3 min in a Fritsch Vibratory Micro Mill Pulverisette 0 to reduce most of the grains to silt size or smaller. These subsamples were then placed in a hollow glass cylinder (~ 40 -mm volume), covered tightly on its bottom end with 4- μ m Ultralene thin-film, and lightly tamped with a flat surfaced tool to reduce porosity (Goff et al., 2020). All subsamples were analyzed in triplicate and the raw elemental data corrected according to in-house linear calibration curves generated from National Institute of Standards and Technology (NIST) standard reference materials (<https://www.nist.gov/srm>; 2701, 2709, 2710, and 8704) (for details, see Schaetzl, Kasmerchak, et al., 2020). The mean value of the three calibrated analyses was considered to be a representative geochemical “signature.” Although the pXRF is capable of measuring a number of major and trace elements (or their oxides), we chose to focus on the distributions of Ca, Fe, Zr, and Ti.

Soil cation exchange capacity (CEC) and extractable cation data for each genetic horizon and the degradational group samples were determined according to the Soil Survey Staff (2014a). The CEC was determined with ammonium acetate buffered at pH 7.0. All CEC subsamples (~ 6 g) were analyzed in triplicate (~ 2 g each), and the mean of the three analyses was used. Extractable base cation contents were determined with ammonium acetate buffered at pH 7.0; after the

initial saturation of the soil with NH_4^+ , the concentration of the four primary displaced basic cations (Ca, Mg, K, and Na) in the extract solution was measured by atomic adsorption spectrophotometry. Standard base cation constant values were used to convert extractable cation data from ppm to $\text{cmol}_c \text{ kg}^{-1}$. Because the parent material here is calcareous and contains “free” carbonates, it was expected that base saturation in horizons that have not experienced significant leaching would be overestimated (i.e., exceed 100%); in such cases, we assumed a base saturation of 100%.

Soil pH values for each horizon were determined using a Mettler MP220 pH meter using a 1:1 water/soil ratio (Soil Survey Staff, 2014a). Each sample was stirred for 30 s at 15-min intervals, and pH readings were taken after 1 h. Soil organic C (SOC) contents for each horizon were determined using loss-on-ignition (LOI) at 430 $^\circ\text{C}$ for 8 h (Nelson & Summer, 1996; Schaetzl, Kasmerchak, et al., 2020; Wang et al., 2012; Wright et al., 2008). We estimated SOC contents (g kg^{-1}) as $\text{LOI}/1.724$, which assumes organic matter is composed of 58% C (Davies, 1974). Lastly, the amounts of amorphous and organically bound Al (Al_{ox}) and Fe (Fe_{ox}), as well as the optical density of the oxalate extract (ODOE), were determined for the upper sequum horizons according to standard ammonium oxalate extraction methods (Soil Survey Staff, 2014a), in order to classify the soil, because the sequum is experiencing podzolization (Schaetzl & Harris, 2011).

A critical component of pedogenic research is the assessment of potential parent material nonuniformity (i.e., the presence of lithologic discontinuities [LDs]; Ahr et al., 2012; Schaetzl, 1998; Schaetzl, Kasmerchak, et al., 2020).

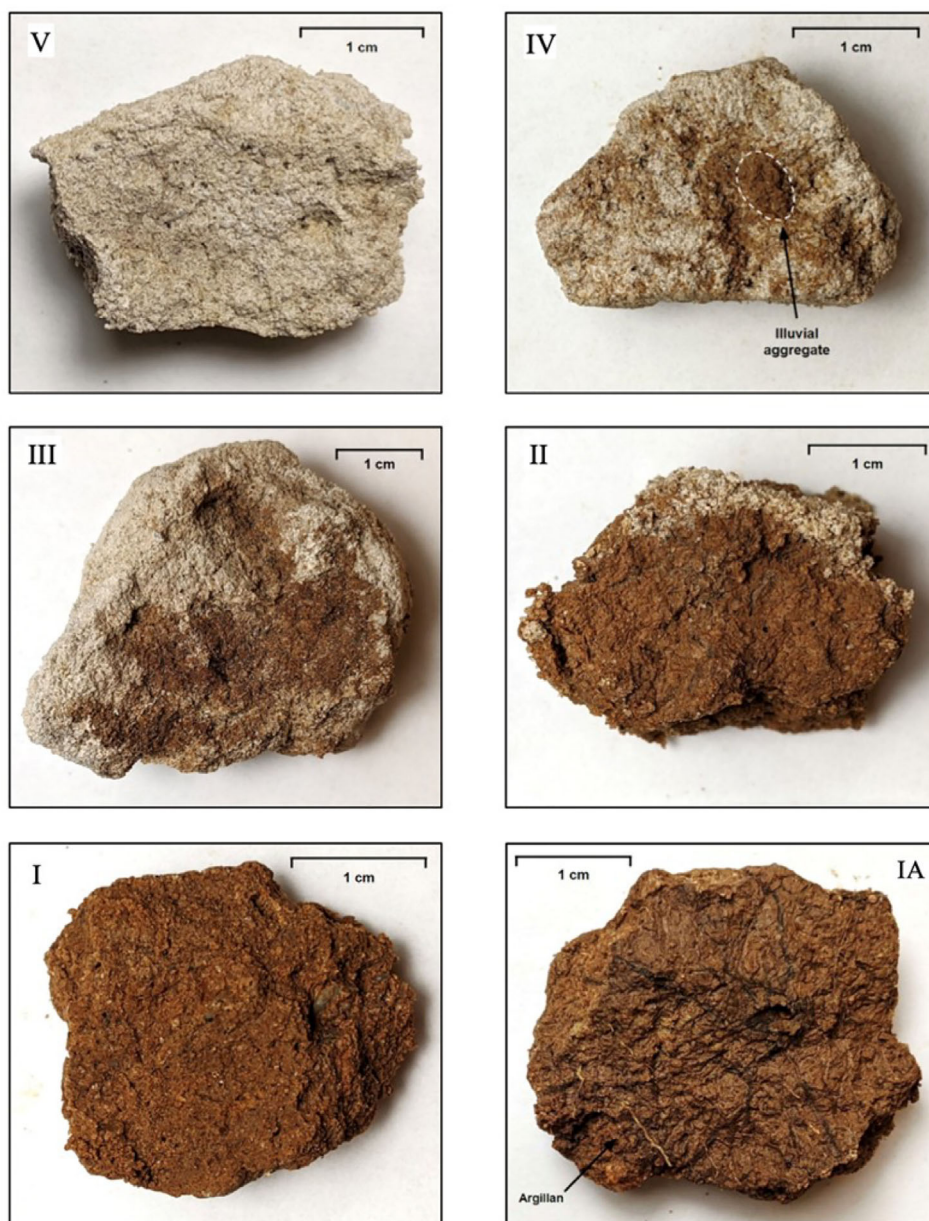


FIGURE 4 Representative examples of intact peds from each glossic horizon group: (V) interior of a completely degraded ped, (IV) interior of a strongly degraded ped, (III) interior of a moderately degraded ped, (II) interior of a weakly degraded ped, (I) interior a nondegraded ped, and (IA) exterior of a nondegraded ped (showing roots proliferating on the ped face). All peds were photographed at 1.7 \times magnification after air drying for 30 min from their initial field moisture condition

Assessment of parent material uniformity is usually done by examining the vertical distribution of immobile particle size separates, particularly sands, and/or slowly weatherable index elements (e.g., Zr and Ti). Because LDs often form as a result of changes in depositional environments, abrupt dissimilarities in the concentration of these components with depth are considered an indicator of parent material nonuniformity (Soil Survey Staff, 2014b). We conducted our evaluation on a pedogenic (mobile) constituent-free basis, so as to not mathematically bias data on the immobile skeletal fraction (Ahr et al., 2012; Soil Survey Staff, 2014b), by focusing on data from the

medium and fine sand subfractions, because of their greater abundance. Additionally, we used Zr and Ti data derived from the pXRF to evaluate index element distribution. It is important to reiterate, however, that geochemical analyses were conducted on the whole-soil material. Thus, we acknowledge the potential for inconsistencies in use of these data, especially Ti (Ahr et al., 2012; Anda et al., 2009; Dąbkowska-Naskręć & Jaworska, 2001; Sudom & Arnaud, 1971), for identification of LDs, particularly in lower profile horizons that have experienced translocation and/or have not undergone significant leaching.

TABLE 2 Morphologic characterization data for the Millersburg pedon

Horizon	Depth cm	Munsell color (moist)	Structure	Consistence		Texture	Boundary	>2 mm est. % (v/v)
				(moist)				
Oi	0–1	–	–	–	–	–	–	–
Oa	1–7	7.5YR 2.5/1	–	–	–	a, s	–	–
E	7–14	7.5YR 5/2	1 f sab	vfr	s	c, w	gravel: 3	
Bs1	14–25	7.5YR 4/6	1 m sab	vfr	ls	c, w	gravel: 3	
Bs2	25–42	7.5YR 5/6	1 m sab	vfr	ls	g, w	gravel: 5	
E/B	42–58	E: 7.5YR 6/3B: 5YR 4/4	2 f-m-c sab	E: vfrB: fr	E: lsB: sl	c, w	gravel: 3	
Bt1	58–72	5YR 4/4	2 m-c sab	fr	sl	c, b	gravel: 3	
Bt2	72–95	5YR 4/6	2 m sab	fr	vs sl	g, w	gravel: 35cobble: 20	
C	95–166+	10YR 5/3	2 m pl	fr	ls	–	gravel: 7cobble: 5	

Note. 1, weak; 2, moderate; f, fine; m, medium; c, coarse; sab, subangular blocky; pl, platy; vfr, very friable; fr, friable; s, sand; ls, loamy sand; sl, sandy loam; vs, very stony; a, abrupt; c, clear; g, gradual; s, smooth; w, wavy; b, broken.

TABLE 3 Physical characterization data for the Millersburg pedon

Horizon	Sand fraction					Silt fraction			Clay	D_b^a g cm ⁻³
	2–1 mm	1–0.5 mm	0.5–0.25 mm	0.25–0.1 mm	0.1–0.05 mm	50–35 μ m	35–25 μ m	25–8 μ m	<8 μ m	
%										
E	0.8	20.6	33.4	21.6	9.8	6.2	2.8	5.5	2.1	1.29 ^b
Bs1	0.6	16.1	29.9	23.3	11.3	6.5	3.1	7.6	4.7	1.29 ^b
Bs2	0.8	19.9	33.8	21.5	8.3	5.8	2.7	5.8	4.1	1.40
E/B	E: 0.5	E: 18.4	E: 33.4	E: 21.0	E: 9.3	E: 4.5	E: 2.1	E: 5.5	E: 7.4	1.47
	B: 0.5	B: 14.8	B: 23.0	B: 15.8	B: 7.8	B: 7.9	B: 4.0	B: 12.7	B: 17.5	
Bt1	0.5	13.0	22.0	16.1	10.5	8.1	3.9	11.9	17.9	1.47
Bt2	0.9	17.9	28.8	19.0	6.8	6.2	3.1	10.0	10.4	0.68
C	0.8	19.0	28.4	19.3	13.6	7.9	3.2	5.4	5.6	1.55

^aBulk density. Values calculated on a stone-free basis.

^bSample taken at E–Bs1 interface due to the thin character of the E horizon.

3 | RESULTS AND DISCUSSION

3.1 | Pedon characterization

The horizonation of the bisqual Millersburg pedon is Oi–Oa–E–Bs1–Bs2–E/B–Bt1–Bt2–C (Figure 3; Table 2). It has a weakly expressed spodic-like (E–Bs1–Bs2) horizon sequence overlying an alfic (E/B–Bt1–Bt2) horizon sequence that shows evidence of a zone of degradation (i.e., a glossic horizon) in its upper portion. Such horizonation is typical of bisqual soils in the Great Lake region containing a glossic horizon (Bockheim, 2015; Schaetzl, 1996). Morphological (Table 2), physical (Table 3), and chemical (Table 4) properties of the pedon indicate that the soil classifies as a coarse-loamy, active, frigid Haplic Glossudalf, and as explained below, is a taxadjunct within the Millersburg series.

Overlying the mineral soil is a thin (<1 cm) surface layer of hardwood leaves, pine needles, and sticks (Oi horizon) above a 6-cm-thick Oa horizon that is black (7.5YR 2.5/1) and very strongly acidic. The underlying E horizon is 7 cm in thickness and brown (7.5YR 5/2) in color. Evidence for strong eluviation in the E horizon is reflected by its sand texture (Figure 5), strongly acidic pH, very low CEC, and considerable (7 cm) thickness. The lack of an A horizon between the E and overlying Oa horizon indicates that bioturbative mixing of organic materials into the mineral soil surface has been negligible. The illuvial portion (Bs1–Bs2 horizons) of the upper sequum has loamy sand textures and strong brown (7.5YR 4/6–5/6) colors. Both were designated Bs horizons in the field because they exhibited evidence of accumulation of sesquioxides and organic matter (i.e., podzolization), as indicated by their high chromas, reddish hues, and similarity to other, weakly developed Spodosols in the region (Schaetzl,

TABLE 4 Chemical characterization data for the Millersburg pedon

Horizon	pH (1:1 H ₂ O)	SOC	CEC	Base sat.	Ca _{total}	Fe _{total}	Zr _{total}	Ti _{total}	Al _{ox}	Fe _{ox}	ODOE
		g kg ⁻¹	cmol _c kg ⁻¹								
Oa	4.9	–	–	–	–	–	–	–	–	–	–
E	5.2	6.5	2.0	45	0.62	1.18	0.06	0.30	0	tr	0.01
Bs1	5.5	12.5	5.3	30	0.63	2.16	0.05	0.28	0.28	0.27	0.17
Bs2	5.8	6.7	2.2	36	0.63	2.07	0.05	0.30	0.19	0.12	0.06
E/B	E: 6.0 B: 7.1	E: 1.8 B: 9.5	4.5	87	0.75	2.29	0.06	0.24	n.d.	n.d.	n.d.
Bt1	7.2	10.7	9.4	100	0.93	3.54	0.06	0.28	n.d.	n.d.	n.d.
Bt2	7.8	5.2	4.8	100	1.68	3.13	0.04	0.18	n.d.	n.d.	n.d.
C	8.6	3.2	2.5	100	7.24	1.43	0.04	0.18	n.d.	n.d.	n.d.

Note. SOC, soil organic C; CEC, cation exchange capacity; Base sat., base saturation; Al_{ox}, organically bound Al; Fe_{ox}, organically bound Fe; ODOE, optical density of the oxalate extract; n.d., not determined.

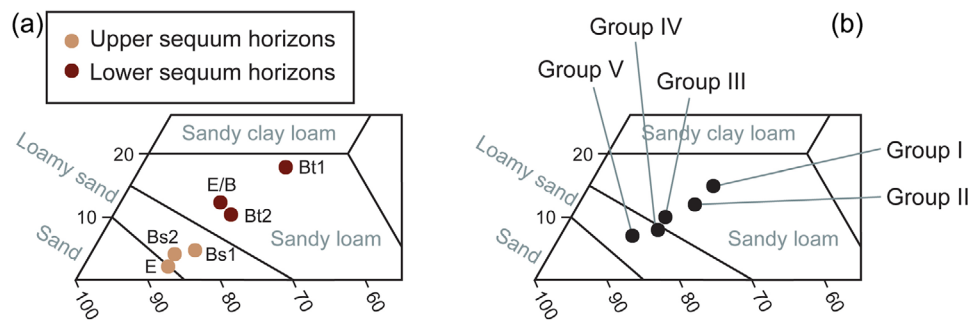


FIGURE 5 Particle-size data for (a) all of the horizons in the Millersburg pedon, and (b) only the glossic (E/B) horizon degradational groups. All data are shown plotted on the lower left portion of a standard Natural Resources Conservation Service (NRCS) textural triangle

1996). Additional chemical indicators, particularly increases in both ODOE values and contents of oxalate extractable Al (Al_{ox}) and Fe (Fe_{ox}), provide quantitative support to this designation. Despite several lines of evidence that podzolization is active and ongoing in the upper sequum, the strength of development of the Bs horizons is insufficient to meet the taxonomic requirements for spodic materials (Soil Survey Staff, 2014b).

Marking the interface between the upper and lower sequa is a well-developed, 16-cm-thick E/B (glossic) horizon (Figure 6). In vertical cross-section, the horizon is composed of ~70% light brown (7.5YR 6/3), degraded, eluvial (albic) soil material (E part) that often coats reddish brown (5YR 4/4), remnant (B part) material. The degraded material occurs on ped margins and along active root channels and macropore pathways. Generally, this material has loamy sand textures (Figure 5), moderately acid pH values, and contains very little SOC. Conversely, the remnant (B part) material has a sandy loam textures, neutral pH values, and contains appreciable SOC. The finer textures in the remnant material occur because of increased clay, and to a lesser

extent, fine silt (8–25 μm), contents. Additional morphological indicators, particularly illuviation cutans bridging primary grains and lining pores, suggest that the clay and fine silt have accumulated by translocation processes (Bockheim &



FIGURE 6 The glossic (E/B) horizon under study here. The knife is ~20 cm long

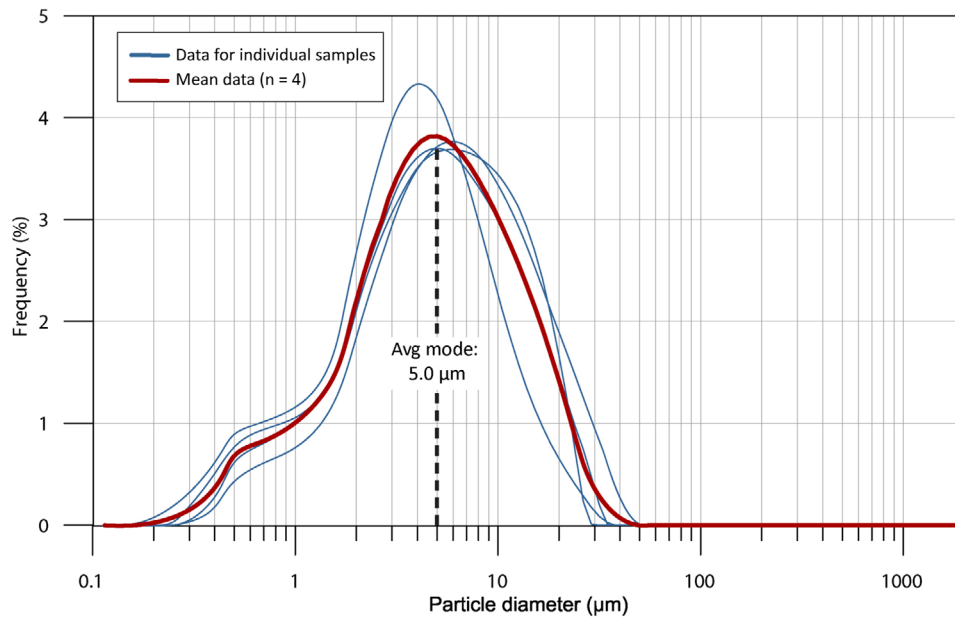


FIGURE 7 Continuous particle size curves for the Bt1 horizon silty-argillans of the Millersburg pedon. Note that, in this study, we are considering the clay–silt break to be at 8 μm

Hartemink, 2013; Phillips, 2004; Soil Survey Staff, 2014b). The glossic horizon has moderate, fine, medium, and coarse subangular blocky structure, parting to moderate fine subangular blocky structure (Table 2). The degree of structural development is largely dependent upon the intensity of degradation, with more strongly degraded peds tending to have finer structure sizes. Furthermore, the more strongly degraded peds tend to have very friable consistence, whereas the more intact peds tend to be friable. Detailed characterization data for the glossic horizon peds at various stages of degradation (as described in Table 1) are provided in Section 3.2. The underlying zone of intact (nondegraded) illuvial material (Bt1 horizon) has reddish brown colors (5YR 4/4), sandy loam textures (Figure 5), and neutral pH values—similar to the remnant (B part) material of the glossic horizon (Tables 2, 3, and 4). Taken together, these data strongly suggest that the two zones are genetically related.

The Bt horizon exhibits abundant evidence of translocation, including illuviation cutans bridging primary grains, lining pores, and coating ped faces. The cutans coating ped faces (i.e., argillans) have a slightly darker reddish brown (5YR 3/4) color than the matrix material (ped interiors), and fine roots tend to proliferate across their surfaces (Figure 4). Particle size data indicate that the argillans are mainly composed ($\sim 72\%$) of clay ($< 8 \mu\text{m}$), and of that, $\sim 72\%$ is in the coarse clay (2–8 μm) subfraction (Figure 7). Virtually all ($\sim 95\%$) of the remaining portion of the argillans is composed of fine silt, approximately half of which occurs within the very fine silt (8–12 μm) subfraction. These data provide a critical supporting line of evidence that both clay and fine silt translocation are occurring contemporaneously in

the pedon. Mixed (clay and silt) illuviation cutans have been referred to as “impure clay coatings” (Bullock & Thompson, 1985; Douglas, 1990; Payton, 1993b; Stoops, 2003); however, for the purpose of clarity, we will refer to these cutans as “silty-argillans.”

The lower boundary of the Bt1 horizon is marked by a layer (Bt2 horizon) dominated by gravel and cobbles (55% by volume), primarily of carbonate lithology. The fine-earth fraction of this horizon has a sandy loam texture (Figure 5) and a yellowish red (5YR 4/6) color (Tables 2 and 3). Similar to the Bt1 horizon, the Bt2 horizon exhibits abundant evidence of translocation, including illuviation cutans bridging primary grains, lining pores, and coating the surfaces of coarse fragments. It is important to note that the content of coarse fragment decreases below the Bt2 horizon, in the C horizon, rendering the Bt2 horizon a morphology much like a “stone zone” (Johnson, 1989; Schaetzl, 1996). Medium and fine sand, as well as Zr, contents in the fine-earth fraction of the Bt2 horizon are, however, comparable with those in the adjacent Bt1 and C horizons. These data indicate that the Bt2 horizon, despite its anomalous concentration of coarse fragments, likely does not represent a zone of contact between materials of distinctly different geologic origin. Because the base of the Bt2 horizon marks the lower boundary of the solum, however, the textural contrast has apparently impeded further vertical advancement of pedogenic processes, particularly translocation, assumedly due to its effect on water flow. Differences in hydraulic tensions between the materials has likely facilitated “hanging” of the wetting front at or near the textural contrast during percolation events, leading to preferential accumulation of translocated materials to form,

and/or reinforce development of, the Bt horizons (Bartelli & Odell, 1960; Khakural et al., 1993; Schaetzl, 1996, 1998).

Pedogenically unaltered parent material (C horizon), identified in the field by strong effervescence with application of dilute HCl, underlies the stone zone. The calcareous nature of the parent material is reflected in its appreciable Ca content and strongly alkaline pH. This material has a platy structure, a loamy sand texture (Figure 5), and is dull yellowish brown (10YR 5/3) in color (Tables 2 and 3). Similar characteristics have been reported for glacial tills of Port Huron age in other northern Michigan locales (Schaetzl, 1996, 2001).

Taxonomically, the soil contains an ochric epipedon that is 14 cm thick, which includes the Oi, Oa, and E horizons. The E horizon classifies as an albic horizon by virtue of its pinkish gray (7.5YR 7/2, dry) color. The E/B horizon, which is 16 cm thick and consists of 70% (by volume) eluvial (E part) material and 30% (by volume) illuvial (B part) material, classifies as a glossic horizon. Additionally, the E portion of the glossic horizon meets the criteria for albic materials by virtue of its light brown (7.5YR 6/3, moist) color. Lastly, the soil contains an argillic horizon that is ~53 cm thick, including the B part of the E/B, Bt1, and Bt2 horizons. Taken together, the diagnostic horizons and properties indicate that the soil classifies as a Haplic Glossudalf (Soil Survey Staff, 2014b). At the family level, the soil control section classifies within the (a) coarse-loamy particle-size class, (b) active cation-exchange activity class, and (c) frigid soil temperature regime. We consider the soil to be a taxadjunct within the Millersburg series due to the lack of an A horizon and presence of the O and Bt2 “stone zone” horizons.

3.2 | Glossic horizon characterization and inferred genesis

The development and occurrence of a glossic horizon is preconditioned by the formation of an argillic (or other clay-enriched) diagnostic subsurface horizon, followed by its subsequent degradation (Soil Survey Staff, 2014b). Working within this paradigm, it can be reasonably assumed that the glossic (E/B) horizon and the immediately subjacent intact (nondegraded) illuvial zone (i.e., the Bt1 horizon) are evolving along similar pedogenic pathways. Thus, the Bt1 horizon serves as a “pedogenic baseline” from which the processes associated with the development and evolution of degraded (eluvial) soil materials in the glossic horizon can be evaluated. Indeed, areas now appearing as glossic features, although likely less strongly developed prior to the onset of degradation due to their pedostratigraphic position, were once the nexus of illuvial accumulation. Thus, we first report on the characteristics of the eluvial (E part) soil materials along the four major degradational phases identified within the glossic (E/B) horizon (Groups II–V). Below, data for these four groups are typi-

cally compared with materials from the Bt1 horizon (Group I; Table 1; Figure 4).

3.3 | Weakly degraded zone (Group II): Initial stages of argillic horizon degradation

The E part of the weakly degraded (Group II) peds represent the initial stage of degradation of the illuvial zone (Table 1; Figure 4). Mean particle size data for these materials indicate that they have sandy loam textures (Figure 5), with 12.2% clay and 16.2% silt (Table 5; Figure 5), representing a net loss of ~21% clay and ~4% silt relative to nondegraded (Group I) peds (Figure 8). The majority (~53%) of the clay loss from the eluvial soil materials is from the fine clay subfraction, indicating that fine clays are preferentially removed during the earliest stages of degradation (Figure 8). The majority (~57%) of the silt loss, albeit relatively negligible overall (0.7% total), has occurred in the fine silt subfraction. The textural coarsening associated with the onset of degradation is assumedly responsible for the large decrease in CEC, from 9.4 to 1.8 cmol_c kg⁻¹ (Figure 9). Taken together, particle size and CEC data indicate that clays remaining in the eluvial soil materials of Group II peds are primarily coarse, likely 1:1 (low activity) clays. Despite the clay loss and associated decrease in CEC, the exchange complex remains saturated with basic cations, mainly Ca (Table 6; Figure 9).

Although it is possible that the base saturation values observed in the eluvial soil materials in Group II peds do not correspond with the conditions during which clay removal occurred, geochemical data indicate that the total Ca content of the materials has decreased by only ~9% relative to Group I peds (Figure 9). Therefore, assuming that the content of “free” Ca in the Bt1 horizon is capable of flocculation and deposition of suspended clays, these data suggest that decarbonation and acidification, although present to some degree, have not been strong enough to facilitate chemical dispersion and eluviation of mobile materials (via desaturation of the exchange complex) from the zone. Geochemical data also reveal a net loss of ~59% total Fe relative to Group I peds (Figure 9), suggesting that its removal (probably as “free” Fe oxides) is likely of greater importance to the remobilization of pedogenic materials, particularly fine clay, than is the desaturation of the exchange complex, during the earliest stages of degradation.

Destabilization and mobilization of Fe oxides in soils, including when in “free” forms associated with illuviation cutans, normally occur under chemically reducing conditions, whereby stable ferric Fe(III) compounds are converted to more soluble ferrous Fe(II) forms (Carroll, 1958; Gotoh & Patrick, 1974). Reducing conditions are initiated as Fe(III) becomes an alternative respiration pathway for microbes and roots after saturation and subsequent limitation of O₂ (Roden,

TABLE 5 Physical characterization data for the E parts of the degradational sequence groups of the Millersburg pedon

Group	Group morphology (overall)	Sand, 2–0.05 mm	Coarse silt, 50–35 μm	Medium silt, 35–25 μm	Fine silt, 25–8 μm	Coarse clay, 8–2 μm	Fine clay, <2 μm
I	Nondegraded material	67.7 \pm 1.4	3.5 \pm 0.1	3.3 \pm 0.2	10.1 \pm 0.5	11.8 \pm 0.5	3.6 \pm 0.1
II (E part)	Weakly degraded material	71.6 \pm 1.6	3.3 \pm 0.2	3.2 \pm 0.2	9.7 \pm 0.5	10.3 \pm 0.6	1.9 \pm 0.1
III (E part)	Moderately degraded material	74.7 \pm 1.5	3.2 \pm 0.3	2.8 \pm 0.2	8.3 \pm 0.4	8.5 \pm 0.5	1.5 \pm 0.1
IV (E part)	Strongly degraded material	79.1 \pm 1.4	2.9 \pm 0.1	2.5 \pm 0.2	7.1 \pm 0.5	7.1 \pm 0.5	1.2 \pm 0.1
V	Completely degraded material	82.6 \pm 1.0	2.3 \pm 0.1	2.1 \pm 0.1	5.5 \pm 0.4	6.3 \pm 0.3	1.1 \pm 0.1

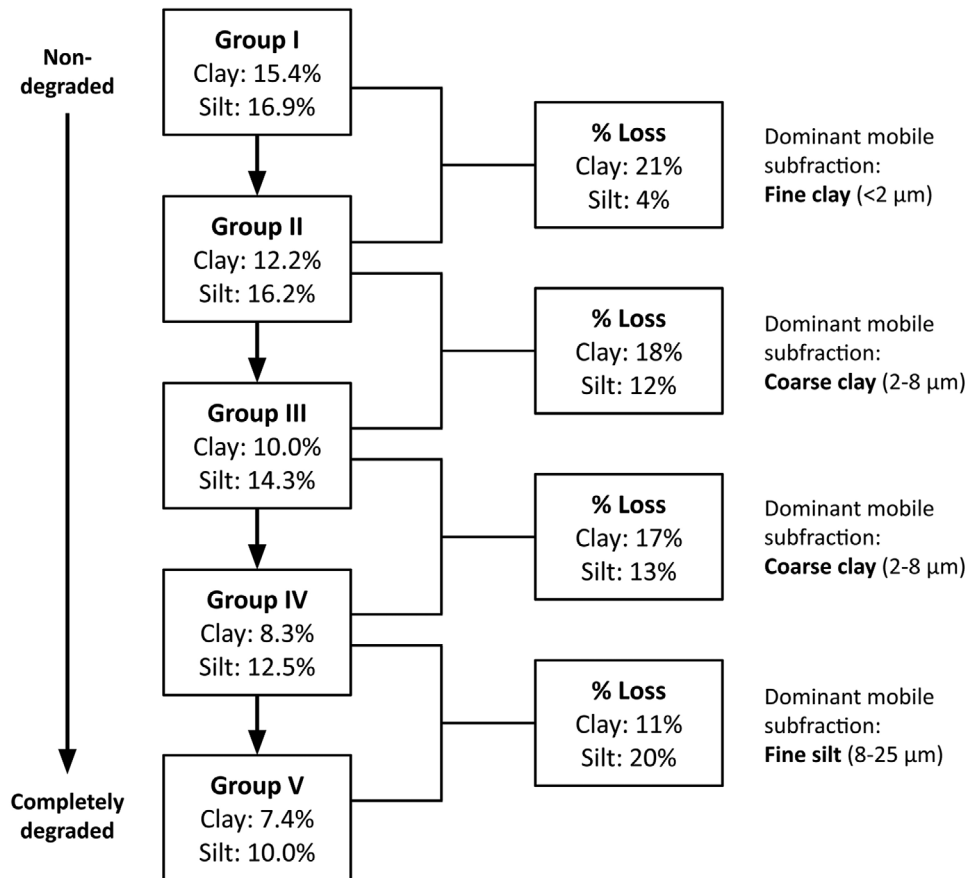


FIGURE 8 Sequential degradation data for eluvial soil materials (E part of peds) of the glossic zone (Groups II–V), relative to nondegraded (Group I) peds

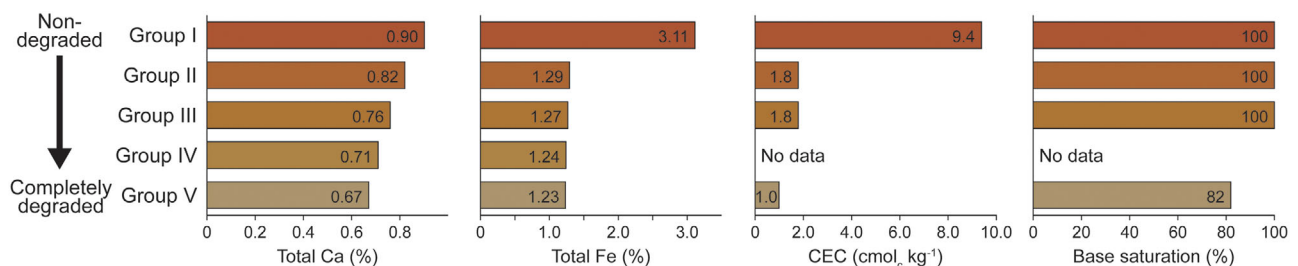


FIGURE 9 Comparative data for total Ca and Fe, cation exchange capacity (CEC), and base saturation of eluvial (E part) soil materials at various stages of degradation in the glossic horizon, relative to nondegraded (Group I) materials. The charts reflect data reported in Table 6

TABLE 6 Chemical characterization data for E parts of the degradational sequence groups of the Millersburg pedon

Group	Group morphology (overall)	Ca _{total}	Fe _{total}	CEC	Base sat.	Extractable cations			
						Ca	Mg	K	Na
		—————%—————		cmol _c kg ⁻¹	%	—————cmol _c kg ⁻¹ —————			
I	Nondegraded material	0.90 ± 0.00	3.11 ± 0.04	9.4	100	7.33	2.16	0.23	0.05
II (E part)	Weakly degraded material	0.82 ± 0.01	1.29 ± 0.03	1.8	100	1.73	0.41	0.08	0.07
III (E part)	Moderately degraded material	0.76 ± 0.02	1.27 ± 0.02	1.8	100	1.43	0.38	0.07	0.10
IV (E part)	Strongly degraded material	0.71 ± 0.00	1.24 ± 0.03	n.d.	n.d.	n.d.	n.d.	n.d.	n.d.
V	Completely degraded material	0.67 ± 0.00	1.23 ± 0.03	1.0	82	0.55	0.18	0.06	0.03

Note. CEC, cation exchange capacity; Base sat., base saturation; n.d., not determined.

2012). However, because the upland soils under study here are coarse-textured and well-drained, they are unlikely to undergo long periods of saturation, as is typical of soils with aquic (or even epiaquic) conditions (Lovley, 1995; Roden, 2012; Soil Survey Staff, 2014b; Weber et al., 2006). Nonetheless, loss of Fe from the upper argillic horizon appears to be a key mechanism responsible for the onset of degradation and, hence, the initiation of glossic development. Thus, it seems reasonable to conclude that redox flux to some degree is in fact occurring, even in these coarse-textured soils.

A growing body of literature is suggesting that reducing conditions can be periodically important in humid, temperate climates, even in well-drained upland soils (De-Campos et al., 2012; Fimmen et al., 2008; Fuss et al., 2010; Hodges et al., 2019; Keiluwet et al., 2016). This research suggests that intermittent pulses of water to the subsoil during seasonally wet periods, particularly when evapotranspiration demands are low and microbial activity is high, are capable of creating ephemeral redox fluctuations and Fe reduction. Generally, these pulses temporarily limit O₂ availability at microsites, even under unsaturated conditions, either through a slowing of O₂ diffusion, or an outpacing of microbial O₂ consumption vs. diffusion. The presence of labile C at such microsites, transported from organic-rich horizons by percolating water and/or derived from roots, further enhances O₂ demand by stimulating microbial activity (De-Campos et al., 2012; Fuss et al., 2010; Hodges et al., 2019). Then, when a O₂ availability becomes insufficient to meet the respiration needs of the microbial community, microbes will use alternative terminal electron acceptors, such as Fe(III) (Hall et al., 2016).

We suggest that the loss of Fe in the Millersburg pedon is driven by its reduction and subsequent eluviation, following a sufficiently large decrease in hydraulic conductivity at the interface of the eluvial-illuvial zone, as suggested in other studies of argillic horizon degradation (Jamagne et al., 1984; Payton, 1993). Wetting fronts, possibly containing appreciable quantities of labile C, may occasionally stop at or near the point of contact between the two texturally contrasting materials, leading to temporarily localized saturation (or situations that approach it) at microsites, followed by fluctuations

in redox status as a result of insufficient O₂. In effect, this event would be a form of short-lived and localized episaturation.

The loss of Fe-rich illuviation cutans generally results in “bleaching” or lightening of the ped faces (Federoff, 1972; Jamagne et al., 1984; Payton, 1993). This process explains the light (7.5YR 6/3) colors of the mobile constituents (i.e., coarse clays and fine silts) remaining in the eluvial soil materials on Group II peds (Figure 4). Notably, soil materials proceeding along the degradational sequence do not express intermediate stages of color change but instead transition from 5YR 4/4 to 7.5YR 6/3 across distances of <1 mm. This pattern attests to the microscales of these areas of temporary saturation and the loss of Fe-rich plasma materials. The bleached, Fe-poor, pedogenic materials that remain become mobile in soil water, having lost their primary binding agents (fine clays and Fe oxides). Thus, they become destabilized and are susceptible to physical detachment from the matrix (i.e., microerosion) and remobilization during subsequent percolation events (Bullock et al., 1974; Jamagne et al., 1984; Payton, 1993).

3.4 | Moderately degraded zone (Group III): Core processes of argillic horizon degradation

The E part of moderately degraded (Group III) peds represents the intermediate stage of degradation of the illuvial zone (Table 1; Figure 4). At this stage, one might describe peds with this morphology as part of a weakly to moderately developed glossic horizon. The boundary between the eluvial soil materials and the underlying matrix (B part) materials tends to be highly diffuse and irregular, indicating uneven encroachment of degradational processes into ped interiors and along preferred percolation pathways (Bullock et al., 1974). Eluvial soil materials also occasionally encroach into macropore flow paths and active root channels within Group III peds, suggesting that, at preferred sites, degradation may also begin to progress from the ped interior outward as this stage is reached.

Mean particle size data for the eluvial (E part) soil materials of Group III indicate that they have sandy loam textures (Figure 5), with 10.0% clay and 14.3% silt (Table 5; Figure 5), representing a net loss of ~35% clay and ~15% silt relative to nondegraded (Group I) peds (Figure 8). At this point, however, the majority (~61%) of the clay loss from the eluvial soil materials is occurring in the coarse clay subfraction. In other words, removal of coarse clays becomes more prominent at this stage, after the initial removal of (mainly) fine clays and associated Fe during earlier periods of degradation (Figure 8). Similarly, removal of silts, albeit remaining subordinate to the removal of coarse clay, also becomes more prominent in intermediate stages of degradation. As would be expected, the majority (~69%) of the observed silt loss at this time is occurring in the fine silt subfraction.

Despite the textural coarsening associated with further degradation, the CEC value of the eluvial (E part) soil materials of Group III peds remains largely unchanged ($1.8 \text{ cmol}_c \text{ kg}^{-1}$) and is accompanied by only a very slight decrease in the total exchangeable cations (Table 6). Thus, the exchange complex remains saturated (100%) with basic cations, mainly Ca. These saturated conditions have been maintained despite the concurrent decrease in total Ca content (~16%), which suggests that decarbonation and acidification become of greater importance by the intermediate stage of degradation. Considering that less clay remains in the eluvial soil materials in the Group III peds, an adequate quantity of “free” Ca likely remains available to saturate the exchange complex. Geochemical data also indicate that only a minor decrease (~2%) in total Fe content has occurred at this point, relative to the eluvial soil materials in Group II peds (i.e., since the initial stage of degradation). Thus, we conclude that, at this point, Fe eluviation is no longer an important component of the degradational process (Figure 9). Instead, other forms of clay and fine silt disaggregation, most likely physical dislodgement and microerosion, assume greater importance.

3.5 | Strongly degraded zone (Group IV): Ending stages of argillic horizon degradation

The E part of strongly degraded (Group IV) peds represents the advanced stage of degradation of the illuvial zone (Table 1; Figure 4). In the field, a contiguous zone of Group IV or similar peds would be viewed as a strongly developed glossic horizon. These materials have loamy sand textures (Figure 5), with mean contents of 8.3% clay and 12.5% silt (Table 5; Figure 5), representing a net loss of ~46% clay and ~26% silt relative to nondegraded (Group I) peds (Figure 8). Similar to what was observed for Group III peds, the majority (~66%) of the observed clay loss from the eluvial soil materials has occurred in the coarse clay subfraction, just as the majority (~68%) of the net silt loss has

occurred in the fine silt subfraction (Figure 8). Although CEC and exchangeable cation data were not collected for eluvial soil materials of Group IV peds, it is likely, based on the observed textural coarsening, that these values have likely decreased relative to the eluvial soil materials of Groups II and III. Geochemical data indicate that the total Ca content of the eluvial soil materials has decreased by ~21%, relative to Group I peds. Geochemical data also indicate that only a minor decrease (~4%) in total Fe content has occurred relative to the eluvial soil materials on Group II peds (Figure 9), suggesting that microerosion remains primarily responsible for further particle remobilization from the degrading zone at the advanced stage of degradation.

3.6 | Completely degraded zone (Group V): Endpoint of argillic horizon degradation

Completely degraded (Group V) peds represent the final stage of degradation of the illuvial zone (Table 1; Figure 4). The presence of isolated flakes of clay on the surfaces of skeletal grains in these peds, occasionally observed under the microscope, indicate that this zone had once been an argillic horizon, as suggested by others (Bullock et al., 1974; Ranney & Beatty, 1969). In essence, Group V peds represent the endpoint to which the illuvial zone is expected to degrade. Thus, if (and when) a laterally contiguous zone (or layer) of such material eventually develops, it would be designated as an E or E' horizon.

Mean particle size data for Group V peds indicate that they have loamy sand textures (Figure 5), with 7.4% clay and 10.0% silt (Table 5), representing a net loss of ~52% clay and ~41% silt relative to nondegraded (Group I) peds (Figure 8). Relative to eluvial soil materials in Group IV peds, these data indicate that fine silt removal supersedes clay removal during the final stages of degradation (Figure 8), providing an additional supporting line of evidence that both clay and fine silts are mobile within these soils. The sum effect of the textural coarsening associated with Bt horizon degradation is assumedly responsible for the very low CEC ($1.0 \text{ cmol}_c \text{ kg}^{-1}$) in the Group V peds—the lowest observed value of any group (Table 6). Despite the clay loss and associated decrease in CEC, the exchange complex remains nearly saturated (86%) with basic cations, mainly Ca. Geochemical data indicate that the total Ca content of Group V peds has decreased by ~30% relative to Group I peds (Figure 9), which suggests that the observed exchangeable acidity is related to desaturation of the exchange complex due to decarbonation and acidification. Geochemical data also indicate that only a minor decrease (~5%) in total Fe content has occurred relative to the eluvial coatings on Group II peds. Taken together, these data indicate that microerosion, and to a lesser extent, desaturation of

the exchange complex, are primarily responsible for particle destabilization and remobilization during the final stages of degradation.

3.7 | New model of glossic horizon genesis

Current theory regarding the genesis of glossic features in coarse-loamy soils in the upper Great Lakes is based largely on dated observations from soils forming under inherently different conditions. Thus, a goal of this study was to develop a conceptual model that provides a more empirical and data-informed explanation for glossic horizon genesis in coarse-textured soils. Our model integrates findings from this study with applicable components of models previously reported in the literature from (a) the upper Great Lakes region, and (b) other locales. Used together, our interpretations provide important insight into (a) the prerequisite conditions influencing glossic profile development, (b) the mechanisms associated with the formation and degradation of the illuvial zone, and as a result, (c) the evolution of glossic horizon morphology.

3.8 | Stage I: Development of the illuvial zone

After deposition of parent material and stabilization of the land surface, incipient pedogenic processes such as littering and melanization, followed by decarbonation and acidification, begin to modify the parent material. In coarse-textured parent materials, especially under non-base-cycling forest vegetation, the acid-neutralizing capacity of the upper solum declines (Cline, 1949; Schaetzl, 1996). Under increasingly acidic conditions, translocation of clay (Bullock et al., 1974; Ranney & Beatty, 1969; Schaetzl, 1996) and fine silt is eventually initiated in the upper profile. Any “free” Fe cations, in various mineralogical forms, derived from the weathering of primary minerals and/or released as a result of litter decay, are complexed by clay minerals, particularly those in the fine clay fraction, which have higher CEC values (Duchaufour & Souchier, 1978). As textural differentiation in the solum progresses, distinct eluvial–illuvial (E–Bt) zones develop and thicken. Due to the calcareous nature of the parent material, deposition of illuvial materials and the formation of a Bt horizon under oxidizing conditions is mainly facilitated by an increase in basic cation content (primarily Ca) on the exchange sites, at depth. Illuvial materials, enriched in various Fe compounds, manifest as reddish (5YR hue) materials in the Bt horizon, enriched in both clay and fine silt. These cutans bridge primary grains, line pores, and coat ped faces. Wetting–drying cycles and microscale bioturbation continually breaks up these incipient illuvial features, such that peds become amalgamations of reddish illuvial materials through-

out the soil matrix (Figure 6). Soon thereafter, as the eluvial zone thickens and acidifies, podzolization is initiated, leading to development and strengthening of bisequal horizonation (Bockheim, 2003; Schaetzl, 1996; Weisenborn & Schaetzl, 2005).

As time progresses, leaching and associated processes, such as decarbonation, acidification, weathering, lessivage, and podzolization, facilitate the gradual downward advancement and thickening of the profile. Pedoturbation is not pronounced at our study site, and as a result, horizon growth and thickening can continue relatively unhindered. Thus, the profile grows downward into fresh parent material, as textural and pH differentiation between the upper and lower sequa become increasingly strong. Progressive textural-finishing of the upper Bt horizon generates a positive feedback loop by fostering increasingly greater dissimilarity in hydraulic tensions between the E and Bt horizons, leading to more frequent wetting front stabilization within the upper Bt horizon or at the E–Bt boundary, enhancing illuvial deposition in the upper portions of the Bt horizon. The Bt horizon grows stronger and its upper boundary deepens, even as the E horizon becomes thicker.

3.9 | Stage II: Initiation of degradation of the illuvial zone

As the Bt horizon becomes increasingly enriched in clay and fine silt, its porosity diminishes, especially in the upper parts of the horizon. The Bt horizon eventually becomes effective as an internal drainage impediment at various microsites. As a result, the duration of temporary, localized saturation (or situations that approach it) in the upper Bt horizon become long enough to foster reducing conditions at microsites, at least occasionally. This process is facilitated not only by wetness or episaturation but also by the high demand for O₂ from roots and microorganisms, which are most common within pores and between peds. At this point, reduction and mobilization of “free” Fe oxides, many of which may be complexed to fine clays in illuviation cutans, becomes favored (Jamagne et al., 1984; Payton, 1993). Under these reducing conditions, even if ephemeral, Fe oxides become soluble and mobile, leaving them susceptible to eluviation, resulting in the bleaching and subsequent destabilization of associated illuviation cutans. As a result, colors of the soil materials make a dramatic shift from 5YR 4/4 to 7.5YR 6/3, due to loss of these Fe-rich materials. The destabilized particles remaining in the cutans (i.e., clays and fine silts) become vulnerable to remobilization via physical dislodgement by percolating water, a process typically referred to as microerosion (Bullock et al., 1974; Jamagne et al., 1984; Payton, 1993). At this time, the degradation of the Bt horizon and the formation of any associated glossic features has begun. From this point forward,

degradational processes become dominant over those associated with further illuvial development but are focused in the upper Bt horizon.

3.10 | Stage III: Evolution of glossic expression

Either occurring contemporaneously with, or immediately after, eluviation of Fe oxides, fine clays are preferentially remobilized from the degrading zone. Our data suggest that Fe oxides (in their various mineralogical forms) serve as a binding agent for the clays and fine silts, and thus their removal leaves these particles vulnerable to dispersion and deflocculation. Reddish (5YR) colors in the Bt horizon (but not in the E and E' parts of the glossic horizon) support this assertion. Glossic features manifest initially as thin, "bleached" eluvial rinds and interfingerings, largely depleted of Fe and fine clay, on ped margins. Similar features have been referred to as pale gray coatings (Cline, 1949), grainy gray ped coatings (Arnold & Riecken, 1964), gray silt coats (Ranney & Beatty, 1969), sugary surface coatings (Bullock et al., 1974), bleached degradation spots (Jamagne et al., 1984), and skeletal surface residues (Payton, 1993).

With each subsequent percolation event, these discrete zones of degradation encroach farther into peds and deeper into the Bt horizon, always along the most permeable conduits, such as those between peds, along macropore flow paths and within active and former root channels. In coarse-textured parent materials, such as those studied here, glossic features may lack the distinctly vertical form and orientation (i.e., tongues) that is typically observed in finer-textured soils (Bullock et al., 1974; Ranney & Beatty, 1969). Instead, materials can be mobilized from areas in the Bt horizon that may not initially appear as ped faces or large pores, due to the more contorted and "open" network of potential flow paths. Thus, degradational features appear to be more "randomly" located and less vertically oriented than in finer-textured soils, where the initial stages of degradation are more focused along clearly defined ped faces (Bullock et al., 1974; Ranney & Beatty, 1969) (Figure 6).

As pedogenic development in the degraded zone progresses to intermediate stages (Figure 4), eluvial rinds on peds become thicker and coarser in texture. Mobilization of these "bleached," destabilized, pedogenic materials, mainly coarse, low-activity clays and to a lesser extent fine silts, drive this process. Although decarbonation and acidification are also occurring at this time, loss of basic cations, particularly Ca, from the degrading zone likely has little influence on particle remobilization at this stage. Base saturation values of 100% in eluvial soil materials support this assertion. Eventually, differentiation of the degrading eluvial-illuvial zone becomes well enough expressed and thick enough that a glos-

sic horizon is formed in the (former) upper part of the Bt horizon.

As degradation progresses into its advanced stages, the increasingly coarse-textured eluvial rinds in the glossic horizon become the dominant matrix component (Figure 4). The only remaining morphological evidence of the former Bt horizon at this stage occurs as isolated, remnant microzones, usually deep in ped interiors. Ultimately, even these illuvial materials are remobilized during the waning stages of degradation. Further loss of Ca from the degraded zone and an increase in exchangeable acidity suggest that acidification and desaturation of the exchange complex, although seemingly remaining subordinate to microerosion, becomes of greater importance at this point. After the Bt horizon becomes completely degraded, it loses all of its former illuvial character. With time, the zone thickens and becomes more contiguous, and structural units become more weakly expressed, until ultimately, it becomes an E or E' horizon.

The pedogenic materials lost during the degradational process are ultimately translocated downward, where they are deposited as fresh, compound cutans in the subjacent Bt horizon (Bullock et al., 1974; Jamagne et al., 1984; Payton, 1993; Ranney & Beatty, 1969). If viewed with only this broad-scale pathway in mind, the soil might be seen as maintaining its original, predominant pedogenic pathway, whereby the eluvial zone gradually advances downward and thickens, just as the illuvial zone concurrently advances downward and thickens (Bullock et al., 1974; Cline, 1949; Ranney & Beatty, 1969). Nonetheless, we point out that along the way, Bt horizon degradation, glossic horizon formation, and E horizon formation are occurring and form the backbone of the pedogenesis in these types of soils.

Finally, we note that in soils where a textural or lithologic change (subtle or obvious) occurs below or within the Bt horizon, such as in this study, this zone may act as an impediment to the vertical advancement pedogenic processes, thereby restricting soil development (partially or completely) within the overlying horizons. Thus, the Bt horizon, while simultaneously acquiring materials from the associated advancing eluvial zone and thereby becoming more strongly expressed, may gradually decrease in thickness, if only for a limited period of time.

4 | CONCLUSIONS

This research documents the importance of redox processes and Fe loss from the Bt horizon as the primary destabilizing triggers for the initiation of glossic feature development in calcareous coarse-textured Udalfs in the upper Great Lakes region; these processes may be more important than the traditionally accepted view of destabilization of clay-rich argillans due to the loss of basic cations from the exchange

complex. We also note that the traditionally defined lessivage that occurs in these soils is associated with not just clay translocation, but also fine silt. These findings have important implications for advancing current theories in soil genesis, including generalized theories of lessivage, as well as enhancing soil classification, and in turn, mapping and management.

Our model of glossic horizon development illustrates and confirms the ways in which this horizon forms, thickens, and grows downward over time. These intra-pedon changes are both predictable and sequential. Further research, using a chronosequence approach to examine glossic horizon development, may provide additional insight into the temporal evolution of the associated pedogenic processes identified and described herein.

Although developed from and for calcareous coarse-textured Glosudalfs in northern Michigan, our interpretations and genetic model may have wider application. That said, our findings may be most applicable to glossic horizons in soils of the northern Great Lakes' states with similar climatic conditions, forest vegetation, parent materials, and deglacial histories. These conditions favor environmental and site factors (e.g., ample precipitation, rapid and unimpeded vertical water percolation to the subsoil [at least occasionally], and wetting–drying of the solum at depth) and pedogenic processes (e.g., decarbonation, acidification, lessivage, episaturation, and related processes) that are conducive to glossic feature genesis. Additionally, our findings may have important implications for explaining glossic feature evolution in soils forming under inherently different conditions, such as in finer-textured parent materials or in soils with fragipans. Most notably, it seems plausible that the initiation of glossic feature development in these soils is also driven by redox processes, especially when an appreciable content of Fe is associated with illuviation cutans, given that the glossic horizon typically exhibits strong texturally contrasting eluvial–illuvial zones. Lastly, it should be noted that glossic horizon formation is supported in soils where pedoturbation is minimal.

The apparent role of temporary saturation or episaturation and associated redox flux in the initiation of argillic horizon degradation raises questions as to the veracity of the taxonomic subgroup classification for Glosudalfs. As currently defined, the condition of temporary saturation or episaturation is recognized only in Aquic and Oxyaquic subgroups of Glosudalfs (Soil Survey Staff, 1999). Similar to the higher-level taxonomic categories, subgroup designations are intended to emphasize the unique attributes and processes that exert primary influence on a soil's evolutionary pathways and development (Soil Survey Staff, 1999). Therefore, in light of our findings, which suggest that periodic saturation or episaturation is likely central to glossic horizon genesis in all Glosudalfs, we advocate that the central concept (i.e., Typic subgroup) be

considered for modification to remove the exclusion on soils that undergo these conditions.

ACKNOWLEDGMENTS

We acknowledge funding support for this research by the Graduate School and Department of Geography, Environment, and Spatial Sciences at Michigan State University, under two separate Graduate Office Fellowship awards made to C.J.B. We thank Alan Arbogast and David Rothstein for their invaluable advice during various phases of this project. We also thank the Kellogg Soil Survey Laboratory, USDA, and the Soil and Plant Nutrient Laboratory, Michigan State University, for laboratory analyses. Lastly, we thank Dr. Kyungsoo Yoo and two anonymous reviewers, whose constructive comments enhanced the quality of this manuscript.


AUTHOR CONTRIBUTIONS

Christopher J. Baish: Conceptualization; Investigation; Methodology; Writing–original draft; Writing–review & editing. Randall J. Schaetzl: Funding acquisition; Supervision; Writing–review & editing.

CONFLICT OF INTEREST

The authors declare no conflict of interest.

ORCID

Randall J. Schaetzl  <https://orcid.org/0000-0002-6070-1365>

REFERENCES

- Ahr, S. W., Nordt, L. C., & Driese, S. G. (2012). Assessing lithologic discontinuities and parent material uniformity within the Texas sandy mantle and implications for archaeological burial and preservation potential in upland settings. *Quaternary Research*, 78, 60–71. <https://doi.org/10.1016/j.yqres.2012.03.013>
- Aide, M., & Aide, C. (2020). Employing geochemical analysis to reveal pedogenic processes in Wisconsin bisequal soils having spodic and alfic sequa. *Journal of Geoscience Research and Environment Protection*, 8, 1–25. <https://doi.org/10.4236/gep.2020.811001>
- Anda, M., Chittleborough, D. J., & Fitzpatrick, R. W. (2009). Assessing parent material uniformity of a red and black soil complex in the landscapes. *Catena*, 79, 142–153. <https://doi.org/10.1016/j.catena.2009.03.011>
- Andresen, J. A., & Winkler, J. A. (2009). Weather and climate. In R. J. Schaetzl, J. T. Darden, & D. Brandt. (Eds.), *Michigan geography and geology* (pp. 288–314). Pearson Custom Publishing.
- Arnold, R. W., & Riecken, F. F. (1964). Grainy gray ped coatings in Brunizem soils. *Proceedings of the Iowa Academy of Sciences*, 71, 350–360.
- Bartelli, L. J., & Odell, R. T. (1960). Field Studies of a clay-enriched horizon in the lowest part of the solum of some Brunizem and Gray-Brown Podzolic soils in Illinois. *Soil Science Society of America Journal*, 24, 388–390. <https://doi.org/10.2136/sssaj1960.03615995002400050024x>

- Blake, G. R., & Hartge, K. H. (1986). Bulk density. In A. Klute (Ed.), *Methods of soil analysis: Part 1. Physical and mineralogical methods* (2nd ed., pp. 363–375). ASA and SSSA. <https://doi.org/10.2136/sssabookser5.1.2ed.c13>
- Blewett, W. L., Winters, H. A., & Rieck, R. L. (1993). New age control on the Port Huron Moraine in northern Michigan. *Physical Geography*, *14*, 131–138. <https://doi.org/10.1080/02723646.1993.10642472>
- Bockheim, J. G. (2003). Genesis of bisequal soils on acidic drift in the upper Great Lakes region, USA. *Soil Science Society of America Journal*, *67*, 612–619. <https://doi.org/10.2136/sssaj2003.6120>
- Bockheim, J. G. (2015). Distribution and origin of glossic horizons in soils of the western Great Lakes region, USA. *Geoderma Regional*, *5*, 226–236. <https://doi.org/10.1016/j.geodrs.2015.08.004>
- Bockheim, J. G., & Hartemink, A. E. (2013). Distribution and classification of soils with clay-enriched horizons in the USA. *Geoderma*, *209*, 153–160. <https://doi.org/10.1016/j.geoderma.2013.06.009>
- Bullock, P., Milford, M. H., & Cline, M. G. (1974). Degradation of argillic horizons in Udalf soils of New York state. *Soil Science Society of America Journal*, *38*, 621–628. <https://doi.org/10.2136/sssaj1974.03615995003800040028x>
- Bullock, P., & Thompson, M. L. (1985). Micromorphology of Alfisols. In L. A. Douglas & M. L. Thompson (Eds.), *Soil micromorphology and soil classification* (Vol. 15, pp. 17–47). SSSA. <https://doi.org/10.2136/sssaspecpub15.c2>
- Burgis, W. A. (1977). *Late-Wisconsinan history of northeastern lower Michigan* (Doctoral dissertation, University of Michigan).
- Carroll, D. (1958). Role of clay minerals in the transportation of iron. *Geochimica et Cosmochimica Acta*, *14*, 1–28. [https://doi.org/10.1016/0016-7037\(58\)90090-5](https://doi.org/10.1016/0016-7037(58)90090-5)
- Cline, M. G. (1949). Profile studies of normal soils of New York: I. Soil profile sequences involving Brown Forest, Gray-Brown Podzolic, and Brown Podzolic soils. *Soil Science*, *68*, 259–272. <https://doi.org/10.1097/00010694-194909000-00006>
- Comer, P. J., Albert, D. A., Wells, H. A., Hart, B. L., Raab, J. B., Price, D. L., Kashian, D. M., Corner, R. A., & Schuen, D. W. (1995). *Michigan's native landscape, as interpreted from the General Land Office surveys 1816–1856. Report to the U.S. E.P.A. Water Division and the Wildlife Division, Michigan Department of Natural Resources*. Michigan Natural Features Inventory.
- Dąbkowska-Naskręt, H., & Jaworska, H. (2001). Titanium in Alfisols formed from glacial deposits of different ages in Poland. *Quaternary International*, *78*, 61–67. [https://doi.org/10.1016/S1040-6182\(00\)00116-6](https://doi.org/10.1016/S1040-6182(00)00116-6)
- Davies, B. E. (1974). Loss-on-ignition as an estimate of soil organic matter. *Soil Science Society of America Proceedings*, *38*, 150–151. <https://doi.org/10.2136/sssaj1974.03615995003800010046x>
- De-Campos, A. B., Huang, C.-H., & Johnston, C. T. (2012). Biogeochemistry of terrestrial soils as influenced by short-term flooding. *Biogeochemistry*, *111*, 239–252. <https://doi.org/10.1007/s10533-011-9639-2>
- Douglas, L. A. (1990). *Soil micromorphology: A basic and applied science*. Elsevier.
- Duchauffour, P., & Souchier, B. (1978). Roles of iron and clay in genesis of acid soils under a humid, temperate climate. *Geoderma*, *20*, 15–26. [https://doi.org/10.1016/0016-7061\(78\)90046-0](https://doi.org/10.1016/0016-7061(78)90046-0)
- Eichenlaub, V. L. (1970). Lake effect snowfall to the lee of the Great Lakes: Its role in Michigan. *Bulletin of the American Meteorological Society*, *51*, 403–413. [https://doi.org/10.1175/1520-0477\(1970\)051%3c0403:LESTTL%3e2.0.CO;2](https://doi.org/10.1175/1520-0477(1970)051%3c0403:LESTTL%3e2.0.CO;2)
- Eshel, G., Levy, G. J., Mingelgrin, U., & Singer, M. J. (2004). Critical evaluation of the use of laser diffraction for particle-size distribution analysis. *Soil Science Society of America Journal*, *68*, 736–743. <https://doi.org/10.2136/sssaj2004.7360>
- Federoff, N. (1972). *Clay illuviation* [Paper presentation]. The 3rd International Working Meeting of Soil Micromorphology, Wrocław, Poland.
- Fimmen, R. L., Richter, D. D., Vasudevan, D., Williams, M. A., & West, L. T. (2008). Rhizogenic Fe–C redox cycling: A hypothetical biogeochemical mechanism that drives crustal weathering in upland soils. *Biogeochemistry*, *87*, 127–141. <https://doi.org/10.1007/s10533-007-9172-5>
- Fisher, P., Aumann, C., Chia, K., O'halloran, N., & Chandra, S. (2017). Adequacy of laser diffraction for soil particle size analysis. *PLOS ONE*, *12*, e0176510. <https://doi.org/10.1371/journal.pone.0176510>
- Fuss, C. B., Driscoll, C. T., Johnson, C. E., Petras, R. J., & Fahey, T. J. (2010). Dynamics of oxidized and reduced iron in a northern hardwood forest. *Biogeochemistry*, *104*, 103–119. <https://doi.org/10.1007/s10533-010-9490-x>
- Goff, K., Schaetzl, R. J., Chakraborty, S., Weindorf, D. C., Kasmerchak, C., & Bettis, E. A. (2020). Impact of sample preparation methods for characterizing the geochemistry of soils and sediments by portable X-ray fluorescence. *Soil Science Society of America Journal*, *84*, 131–143. <https://doi.org/10.1002/saj2.20004>
- Gotoh, S., & Patrick, W. H. (1974). Transformation of iron in a waterlogged soil as influenced by redox potential and pH. *Soil Science Society of America Journal*, *38*, 66–71. <https://doi.org/10.2136/sssaj1974.03615995003800010024x>
- Hall, S. J., Liptzin, D., Buss, H. L., Deangelis, K., & Silver, W. L. (2016). Drivers and patterns of iron redox cycling from surface to bedrock in a deep tropical forest soil: A new conceptual model. *Biogeochemistry*, *130*, 177–190. <https://doi.org/10.1007/s10533-016-0251-3>
- Harpstead, M., & Rust, R. H. (1964). A pedological characterization of five profiles in gray wooded soils area of Minnesota. *Soil Science Society of America Journal*, *18*, 113–118. <https://doi.org/10.2136/sssaj1964.03615995002800010046x>
- Henne, P. D., & Hu, F. S. (2010). Holocene climatic change and the development of the lake-effect snowbelt in Michigan, USA. *Quaternary Science Reviews*, *29*, 940–951. <https://doi.org/10.1016/j.quascirev.2009.12.014>
- Hodges, C., Mallard, J., Markewitz, D., Barcellos, D., & Thompson, A. (2019). Seasonal and spatial variation in the potential for iron reduction in soils of the Southeastern Piedmont of the US. *Catena*, *180*, 32–40. <https://doi.org/10.1016/j.catena.2019.03.026>
- Hole, F. D. (1975). Some relationships between forest vegetation and Podzol B horizons in soils of Menominee tribal lands, Wisconsin, USA. *Soviet Soil Science*, *7*, 714–723.
- International Union of Soil Sciences (IUSS) Working Group WRB (2015). *World Reference Base for soil resources 2014, update 2015. International soil classification system for naming soils and creating legends for soil maps* (World Soil Resources Reports No. 106). Food and Agriculture Organization.
- Isard, S. A., & Schaetzl, R. J. (1995). Estimating soil temperatures and frost in the lake effect snowbelt region, Michigan, USA. *Cold Regions Science and Technology*, *23*, 317–332. [https://doi.org/10.1016/0165-232X\(94\)00020-X](https://doi.org/10.1016/0165-232X(94)00020-X)
- Jamagne, M., De Coninck, F., Robert, M., & Maucorps, J. (1984). Mineralogy of clay fractions of some soils on loess in northern France. *Geoderma*, *33*, 319–342. [https://doi.org/10.1016/0016-7061\(84\)90032-6](https://doi.org/10.1016/0016-7061(84)90032-6)

- Johnson, D. L. (1989). Subsurface stone lines, stone zones, artifact-manuport layers, and biomantles produced by bioturbation via pocket gophers (*Thomomys bottae*). *American Antiquity*, *54*, 370–389. <https://doi.org/10.2307/281712>
- Keiluweit, M., Nico, P. S., Kleber, M., & Fendorf, S. (2016). Are oxygen limitations under recognized regulators of organic carbon turnover in upland soils? *Biogeochemistry*, *127*, 157–171. <https://doi.org/10.1007/s10533-015-0180-6>
- Khakural, B. R., Lemme, G. D., & Mokma, D. L. (1993). Till thickness and argillic horizon development in some Michigan Hapludalfs. *Soil Survey Horizons*, *34*, 6–13. <https://doi.org/10.2136/sh1993.1.0006>
- Konert, M., & Vandenberghe, J. (1997). Comparison of laser grain size analysis with pipette and sieve analysis: A solution for the underestimation of the clay fraction. *Sedimentology*, *44*, 523–535. <https://doi.org/10.1046/j.1365-3091.1997.d01-38.x>
- Krist, F. K., & Lusch, D. P. (2004). Glacial history of Michigan, U.S.A: A regional perspective. *Developments in Quaternary Sciences*, *2*, 111–117. [https://doi.org/10.1016/S1571-0866\(04\)80191-X](https://doi.org/10.1016/S1571-0866(04)80191-X)
- Lovley, D. R. (1995). Microbial reduction of iron, manganese, and other metals. *Advances in Agronomy*, *54*, 175–231. [https://doi.org/10.1016/S0065-2113\(08\)60900-1](https://doi.org/10.1016/S0065-2113(08)60900-1)
- Miller, B. A., & Schaetzl, R. J. (2012). Precision of soil particle size analysis using laser diffractometry. *Soil Science Society of America Journal*, *76*, 1719–1727. <https://doi.org/10.2136/sssaj2011.0303>
- Nelson, D. W., & Sommers, L. E. (1996). Total carbon, organic carbon, and organic matter. In D. L. Sparks, et al. (Eds.), *Methods of soil analysis. Part 3. Chemical methods* (pp. 961–1010). ASA and SSSA. <https://doi.org/10.2136/sssabookser5.3.c34>
- Nyland, K. E., Schaetzl, R. J., Ignatov, A., & Miller, B. A. (2018). A new depositional model for sand-rich loess on the Buckley Flats outwash plain, northwestern Lower Michigan. *Aeolian Research*, *31*, 91–104. <https://doi.org/10.1016/j.aeolia.2017.05.005>
- Payton, R. W. (1993). Fragipan formation in argillic brown earths (Fragiudalfs) of the Milfield Plain, north-east England. III. Micromorphological, SEM and EDXRA studies of fragipan degradation and the development of glossic features. *Journal of Soil Science*, *44*, 725–729. <https://doi.org/10.1111/j.1365-2389.1993.tb02335.x>
- Phillips, J. D. (2004). Geogenesis, pedogenesis, and multiple causality in the formation of texture-contrast soils. *Catena*, *58*, 275–295. <https://doi.org/10.1016/j.catena.2004.04.002>
- Purkey, T. H. C. (2003). *Soil survey of Montmorency County, Michigan*. U.S. Government Printing Office.
- Ranney, R. W., & Beatty, M. T. (1969). Clay translocation and albic tongue formation in two Glossoboralfs of west-central Wisconsin. *Soil Science Society of America Journal*, *33*, 768–775. <https://doi.org/10.2136/sssaj1969.03615995003300050040x>
- Roden, E. E. (2012). Microbial iron-redox cycling in subsurface environments. *Biochemical Society Transactions*, *40*, 1249–1256. <https://doi.org/10.1042/BST20120202>
- Schaetzl, R. J. (1996). Spodosol-Alfisol intergrades: Bisequal soils in NE Michigan, USA. *Geoderma*, *74*, 23–47. [https://doi.org/10.1016/S0016-7061\(96\)00060-2](https://doi.org/10.1016/S0016-7061(96)00060-2)
- Schaetzl, R. J. (1998). Lithologic discontinuities in some soils on drumlins: Theory, detection, and application. *Soil Science*, *163*, 570–590. <https://doi.org/10.1097/00010694-199807000-00006>
- Schaetzl, R. J. (2001). Late Pleistocene ice flow directions and the age of glacial landscapes in northern lower Michigan. *Physical Geography*, *22*, 28–41. <https://doi.org/10.1080/02723646.2001.10642728>
- Schaetzl, R. J. (2008). The distribution of silty soils in the Grayling Fingers region of Michigan: Evidence for loess deposition onto frozen ground. *Geomorphology*, *102*, 287–296. <https://doi.org/10.1016/j.geomorph.2008.03.012>
- Schaetzl, R. J., Baish, C., Colgan, P. M., Knauff, J., Bilintoh, T., Wanyama, D., Church, M., Mckeehan, K., Fulton, A., & Arbogast, A. F. (2020). A sediment-mixing process model of till genesis, using texture and clay mineralogy data from Saginaw Lobe (Michigan, USA) tills. *Quaternary Research*, *94*, 174–194. <https://doi.org/10.1017/qua.2019.82>
- Schaetzl, R. J., Enander, H., Luehmann, M. D., Lusch, D. P., Fish, C., Bigsby, M., Steigmeyer, M., Guasco, J., Forgacs, C., & Pollyea, A. (2013). Mapping the physiography of Michigan using GIS. *Physical Geography*, *34*, 1–38. <https://doi.org/10.1080/02723646.2013.778531>
- Schaetzl, R. J., & Harris, W. (2011). Spodosols. In P. M. Huang, Y. Li, & M. E. Sumner (Eds.), *Handbook of soil sciences: Properties and processes* (2nd ed., pp. 33–113–33–127). CRC Press.
- Schaetzl, R. J., & Isard, S. A. (1991). The distribution of Spodosol soils in southern Michigan: A climatic interpretation. *Annals of the Association of American Geographers*, *81*, 425–442. <https://doi.org/10.1111/j.1467-8306.1991.tb01703.x>
- Schaetzl, R. J., Kasmerchak, C., Šamonil, P., Baish, C., Hadden, M., & Rothstein, D. E. (2020). Acidification and weathering associated with deep tongues in sandy Spodosols, Michigan, USA. *Geoderma Regional*, *23*, e00332. <https://doi.org/10.1016/j.geodrs.2020.e00332>
- Schoeneberger, P. J., Wysocki, D. A., & Benham, E. C., & Soil Survey Staff. (2012). *Field book for describing and sampling soils* (Version 3.0). National Soil Survey Center.
- Schumacher, B. A., Shines, K. C., Burton, J. V., & Papp, M. L. (1990). Comparison of three methods for soil homogenization. *Soil Science Society of America Journal*, *54*, 1187–1190. <https://doi.org/10.2136/sssaj1990.03615995005400040046x>
- Soil Survey Staff. (1999). *Soil taxonomy: A basic system of soil classification for making and interpreting soil surveys* (2nd ed.). USDA-NRCS.
- Soil Survey Staff. (2014a). *Kellogg Soil Survey laboratory methods manual* (Soil Survey Investigations Report 42, Version 5.0). USDA-NRCS.
- Soil Survey Staff. (2014b). *Keys to soil taxonomy* (12th ed.). USDA-NRCS.
- Stoops, G. (2003). *Guidelines for analysis and description of soil and regolith thin sections*. SSSA.
- Sudom, M. D., & St Arnaud, R. J. (1971). Use of quartz, zirconium and titanium as indices in pedological studies. *Canadian Journal of Soil Science*, *51*, 385–396. <https://doi.org/10.4141/cjss71-052>
- Wang, X., Wang, J., & Zhang, J. (2012). Comparisons of three methods for organic and inorganic carbon in calcareous soils of northwestern China. *PLOS ONE*, *7*, e44334. <https://doi.org/10.1371/journal.pone.0044334>
- Weber, K. A., Achenbach, L. A., & Coates, J. D. (2006). Microorganisms pumping iron: Anaerobic microbial iron oxidation and reduction. *Nature Reviews Microbiology*, *4*, 752–764. <https://doi.org/10.1038/nrmicro1490>
- Weisenborn, B. N., & Schaetzl, R. J. (2005). Range of fragipan expression in some Michigan soils: I. Morphological, micromorphological, and pedogenic characterization. *Soil Science Society of America Journal*, *69*, 168–177. <https://doi.org/10.2136/sssaj2005.0168>

- Whitney, G. G. (1987). An ecological history of the Great Lakes forest of Michigan. *Journal of Ecology*, 75, 667–684. <https://doi.org/10.2307/2260198>
- Wright, A. L., Wang, Y.u., & Reddy, K. R. (2008). Loss-on-ignition method to assess soil organic carbon in calcareous Everglades wetlands. *Communications in Soil Science and Plant Analysis*, 39, 3074–3083. <https://doi.org/10.1080/00103620802432931>
- Yang, Y., Wang, L., Wendroth, O., Liu, B., Cheng, C., Huang, T., & Shi, Y. (2019). Is the laser diffraction method reliable for soil particle size distribution analysis? *Soil Science Society of America Journal*, 83, 276–287. <https://doi.org/10.2136/sssaj2018.07.0252>

How to cite this article: Baish, C. J., Schaetzl, R. J. New insights into the origin and evolution of glossic features in coarse-textured soils in northern lower Michigan (USA). *Soil Sci Soc Am J.* 2021;85:2115–2134. <https://doi.org/10.1002/saj2.20331>